

Collision Avoidance for Non-Cooperative Multi-Swarm Coverage Control with Bounded Disturbance Measurements

Karolina Schmidt and Luis Rodrigues

Department of Electrical and Computer Engineering

Concordia University, Montréal, QC, Canada

Email: karolina.schmidt@mail.concordia.ca, luis.rodrigues@concordia.ca

Abstract— This paper proposes a new algorithm for collision-free coverage control of multiple non-cooperating swarms in the presence of bounded disturbances. A new methodology is introduced that accounts for uncertainties in disturbance measurements. The proposed methodology is used to develop an algorithm that ensures collision-free motion in multi-swarm coverage control, specifically for cases where disturbances are present and their measurements are subject to bounded uncertainty. The theoretical results are validated through simulations of multiple swarms that independently aim to cover a given region in an environment with disturbances.

Index Terms— Coverage control, multi-agent systems, collision avoidance, disturbance

Notice to practitioners— The motivation of this paper arises from the increased use of multi-agent systems over the past years, which has led to a need to operate multiple independent swarms within shared spaces. As outlined in the introduction section, examples include wildfire management, planetary exploration, and mobile coverage provided by drones. Important considerations to ensure safe motion are the avoidance of collisions between agents, as well as the compensation for disturbances, such as winds or currents, and uncertainty in their measurements. This paper proposes a new methodology for multi-agent collision avoidance with disturbance measurement uncertainty and mathematically guarantees collision-free motion. While the methodology can be used for general types of multi-agent systems, we propose a new algorithm that incorporates the collision avoidance methodology into coverage control with multiple non-cooperating swarms. Three-dimensional simulations show that, despite collision avoidance maneuvers, maximum coverage is achieved by all swarms.

I. INTRODUCTION

Due to the various tasks that swarms of agents are intended to execute, there is a need for multiple non-cooperating swarms to independently provide maximum coverage to a common region. In these scenarios, agents need to avoid collisions while compensating for unintended drifts caused by disturbances. Examples include wind drift for Unmanned Aerial Vehicles (UAVs) or currents in scenarios involving Autonomous Underwater Vehicles (AUVs). Applications for the provision of coverage with multiple non-cooperating swarms are search and rescue while simultaneously performing fire monitoring, planetary exploration where swarms belonging to different countries independently aim to cover as much terrain as possible, as well as mobile coverage in remote areas provided by drones from different companies. Motivated by these applications we propose an uncertainty-aware collision avoidance approach for multi-agent systems and apply it to coverage control with multiple non-

cooperating swarms. The focus of the paper is on bounded uncertainties in the measurement of disturbances. Preliminary work by the same authors for the disturbance-free two-dimensional problem can be found in reference [1].

Coverage control using centroidal Voronoi configurations was first investigated by Cortés et al. in references [2], [3]. Using Lloyd’s iterative algorithm [4] and gradient descent methods, a swarm of agents is coordinated to provide maximum coverage for a region. Extensions and further advancements are proposed in reference [5] where energy conservation and efficiency are considered by formulating an optimal control problem. Moreover, reference [6] introduces an analytic expression for the rate of change of the mass and the location of the center of mass of a Voronoi cell, while the authors in [7] address the problem introduced in [5] for discrete-time systems. More recent work addresses obstacle avoidance in coverage control using control barrier functions [8], [9], leader-follower approaches [10], as well as ant colony algorithms [11]. Position uncertainty in collision-free coverage control is addressed in [12] and [13], while [14] considers system uncertainty. Various papers [15]–[19] consider more than one swarm of agents in different scenarios. These include formation flying [15], collaborative coverage control of UAVs and Unmanned Ground Vehicles [16], time-efficient coverage control with cooperating swarms using a leader-follower approach [17], and the division of a swarm into sub-groups to increase coverage speed and reduce traveling distances [18] or to deploy heterogeneous agents [19]. A review of coverage control algorithms is given in [20].

A widely studied approach to avoid moving obstacles for robot motion is the Velocity Obstacles (VO) method presented in [21]. Extensions and improvements include [22] and [23], where collision-free motion for multi-agent systems is addressed. Reference [24] introduces a geometric approach called Optimal Reciprocal Collision Avoidance (ORCA) allowing the agents to solve a low-dimensional linear program to compute collision-free velocities. A detailed overview of VO-based collision avoidance methods is given in [25]. Uncertainty in the position and velocity of obstacles in collision avoidance methods based on Velocity Obstacles is addressed in [26]–[29]. Reference [30] presents risk-bounded motion planning using Velocity Obstacles with disturbances, Gaussian sensor noise, and model uncertainty. Nevertheless, none of the above references considers the effects of uncertainty in the measurements of disturbances. Independent of

Velocity Obstacles and its extensions, reference [31] analyzes parameters in obstacle avoidance under the presence of wind.

To the best of the authors' knowledge, reference [1] is the only work that considers the scenario of multiple non-cooperating swarms that independently aim to cover a common region while avoiding collisions among agents, but it does not consider uncertainty. Moreover, the reference only considers planar motion of the agents, so that collision avoidance maneuvers are only performed in two dimensions. This can be a limiting factor when the agents are UAVs or AUVs. The contributions of this paper are the following:

- 1) A methodology for collision-free motion in multi-agent scenarios accounting for uncertainty in the measurement of bounded disturbances is proposed. Formal guarantees for collision avoidance are derived.
- 2) A new algorithm for collision-free coverage control with multiple non-cooperating swarms accounting for bounded disturbances and uncertainty in their measurements is proposed. Simulations are shown for three-dimensional motion, thus enabling UAV and AUV applications.

Notice that contribution 1 is not specific to non-cooperative multi-swarm coverage control as the method can be used for general types of multi-agent systems. It extends ORCA to the case of bounded disturbances with measurement uncertainty.

The paper is organized as follows. Section II summarizes preliminaries on coverage control and ORCA. The proposed methodology to account for uncertainties in the measurements of disturbances is introduced and formulated in section III. It is then used to propose an algorithm for multi-swarm coverage control that is presented in section III-C. Three-dimensional simulations are shown in section IV, before conclusions are drawn in section V.

II. PRELIMINARIES

A. Energy-Efficient Coverage Control

This subsection follows references [2], [3], [5]. Let Q be a convex region and let n agents be located at distinct positions $X = \{x_1, \dots, x_n\}$, where $x_i \in Q, i \in \{1, \dots, n\}$. Then, using Voronoi tessellation, Q can be divided into subsets called Voronoi cells V_i so that each point $q \in Q$ is associated with the closest agent, i.e., $V_i(X) = \{q \in Q \mid \|q - x_i\|_2 \leq \|q - x_j\|_2 \forall x_j \in X\}$. A distance function for a point $q \in Q$ is described as $f(x_{i(q)}, q) = \|x_{i(q)} - q\|$, where $x_{i(q)}$ is the position of the closest agent to q . High distance values correspond to a low level of coverage, while low values indicate high coverage. The importance of coverage at q is described by a density function $\phi(q)$. Therefore, to maximize coverage the following function is minimized [5],

$$V(x) = \sum_{i=1}^n \int_{V_i} \|x_i - q\|^2 \phi(q) dq. \quad (1)$$

Using the necessary condition for a local minimum yields

$$\frac{\partial V}{\partial x_i} = 2M_{V_i}(x_i - CM_{V_i})^T = 0, \quad (2)$$

where M_{V_i} is the mass and CM_{V_i} is the center of mass of Voronoi cell V_i , written as

$$M_{V_i} = \int_{V_i} \phi(q) dq, \quad (3)$$

$$CM_{V_i} = \frac{\int_{V_i} q \phi(q) dq}{\int_{V_i} \phi(q) dq} = \frac{\int_{V_i} q \phi(q) dq}{M_{V_i}}. \quad (4)$$

Equation (2) is satisfied when $x_i = CM_{V_i}$. A configuration where each agent is located at the center of mass of its Voronoi cell is called a centroidal Voronoi configuration. Lloyd's iterative algorithm [4] can be used to move each agent towards the center of mass of its Voronoi cell.

The authors of [5] formulate the efficient coverage task as the following optimal control problem,

$$\inf_{u_i, i \in \{1, \dots, n\}} \int_0^\infty \sum_{i=1}^n \left(s_i \left\| \int_{V_i} (x_i - q) \phi(q) dq \right\|^2 + r_i u_i^T u_i \right) d\tau$$

$$s.t. \dot{x}_i = u_i, \quad (5)$$

where u_i is the control input of agent i . The coefficients $s_i \geq 0$ and $r_i > 0$ weigh the importance of coverage as measured by

$$M_{V_i} \|x_i - CM_{V_i}\| = \left\| \int_{V_i} (x_i - q) \phi(q) dq \right\| \quad (6)$$

and input energy for each agent, respectively. The authors in [5] prove that a solution of (5) is

$$u_i = -\sqrt{s_i/r_i} \int_{V_i} (x_i - q) \phi(q) dq. \quad (7)$$

A first order dynamical model for the closed-loop dynamics of each agent is thus

$$\dot{x}_i = u_i, \quad (8)$$

$$u_i = k_i (CM_{V_i} - x_i),$$

where $k_i = M_{V_i} \sqrt{s_i/r_i}$.

B. Optimal Reciprocal Collision Avoidance (ORCA)

This subsection follows reference [24]. Consider two spherical agents A and B with radii r_A and r_B and centered at positions x_A and x_B , respectively.

Definition 1. A collision between two spherical agents A and B occurs, when

$$\|x_A - x_B\| \leq r_A + r_B. \quad (9)$$

Conversely, the agents do not collide when

$$\|x_A - x_B\| > r_A + r_B. \quad (10)$$

Using ORCA, agent A can compute a truncated collision cone in the velocity space denoted as \mathcal{VO}_{AB}^τ and called the Velocity Obstacle of A with respect to B for time horizon τ . The Velocity Obstacle \mathcal{VO}_{AB}^τ is computed as [24]

$$\mathcal{VO}_{AB}^\tau = \{v \mid \exists t \in (0, \tau] : v \in S((x_B - x_A)/t, (r_A + r_B)/t)\}, \quad (11)$$

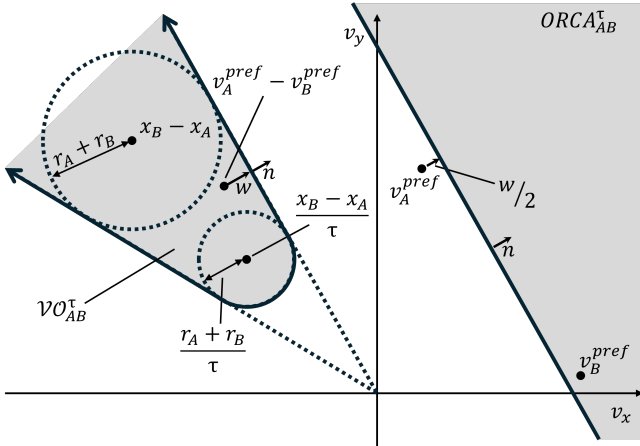


Fig. 1: Geometry of \mathcal{VO}_{AB}^{τ} , adapted from [24]

where S describes a sphere,

$$S(x, r) = \{q \mid \|q - x\| \leq r\}. \quad (12)$$

The set \mathcal{VO}_{AB}^{τ} in two dimensions is shown in figure 1.

Theorem 1. ([32], page 24) Consider two agents A and B traveling with velocities v_A and v_B , respectively. Let both v_A and v_B be constant for a time horizon τ . Then, A and B collide within the time horizon τ if and only if

$$v_A - v_B \in \mathcal{VO}_{AB}^{\tau}. \quad (13)$$

Therefore, A and B do not collide if and only if

$$v_A - v_B \notin \mathcal{VO}_{AB}^{\tau}. \quad (14)$$

Let v_A^{pref} and v_B^{pref} be the desired velocities that A and B aim to follow, respectively, to meet other potential path planning objectives. To avoid a collision with B, A computes the shortest vector w from

$$v_{AB}^{\text{pref}} = v_A^{\text{pref}} - v_B^{\text{pref}} \quad (15)$$

to the boundary of \mathcal{VO}_{AB}^{τ} , denoted as $\partial \mathcal{VO}_{AB}^{\tau}$ [24],

$$w = \left(\underset{v \in \partial \mathcal{VO}_{AB}^{\tau}}{\text{argmin}} \|v - v_{AB}^{\text{pref}}\| \right) - v_{AB}^{\text{pref}}. \quad (16)$$

Assuming that A and B share the responsibility to avoid each other, both agents compute a half-space containing velocities that they can adopt so that, if both A and B keep their velocities constant during a time horizon τ , the two agents do not collide with each other within τ instants of time. The half-space of agent A with respect to B is described as [24]

$$\text{ORCA}_{AB}^{\tau} = \left\{ v \mid \left(v - \left(v_A^{\text{pref}} + \frac{1}{2}w \right) \right) \cdot n > 0 \right\}, \quad (17)$$

where n is the outward normal vector of $\partial \mathcal{VO}_{AB}^{\tau}$ at $v_{AB}^{\text{pref}} + w$. The half-space of agent B with respect to A is

$$\text{ORCA}_{BA}^{\tau} = \left\{ v \mid \left(v - \left(v_B^{\text{pref}} - \frac{1}{2}w \right) \right) \cdot (-n) > 0 \right\}. \quad (18)$$

Notice that the boundary of ORCA_{BA}^{τ} is parallel to that of ORCA_{AB}^{τ} , but the corresponding normal vector points in the opposite direction.

Theorem 2. ([32], page 33) Consider an agent A and an agent B. Let A adopt any velocity $v_A^{\text{new}} \in \text{ORCA}_{AB}^{\tau}$ and let B adopt any velocity $v_B^{\text{new}} \in \text{ORCA}_{BA}^{\tau}$. If v_A^{new} and v_B^{new} are constant for a time horizon τ , then A and B do not collide before τ , i.e.,

$$v_A^{\text{new}} - v_B^{\text{new}} \notin \mathcal{VO}_{AB}^{\tau}. \quad (19)$$

In multi-agent scenarios with m agents, the set of feasible velocities for A is obtained by computing a half-space with respect to each other agent B_1, \dots, B_{m-1} along with a sphere $S(0, v_A^{\text{max}})$, where v_A^{max} is the maximum speed achievable by A. Taking the intersection of all half-spaces computed by A and $S(0, v_A^{\text{max}})$ yields

$$\text{ORCA}_A^{\tau} = S(0, v_A^{\text{max}}) \cap \bigcap_{i=1}^{m-1} \text{ORCA}_{AB_i}^{\tau}. \quad (20)$$

Corollary 1. ([32], page 35) Consider m agents operating within the same area and following the ORCA approach to avoid collisions with each other. Then an agent A choosing its new velocity $v_A^{\text{new}} \in \text{ORCA}_A^{\tau}$, where

$$\text{ORCA}_A^{\tau} = S(0, v_A^{\text{max}}) \cap \bigcap_{i=1}^{m-1} \text{ORCA}_{AB_i}^{\tau}, \quad (21)$$

will not collide with any other agent $B_i, i \in \{1, \dots, m-1\}$, before a time horizon τ , if $v_{B_i}^{\text{new}} \in \text{ORCA}_{B_i}^{\tau}$, assuming that v_A^{new} and $v_{B_i}^{\text{new}}$ are constant for τ , i.e.,

$$v_A^{\text{new}} - v_{B_i}^{\text{new}} \notin \mathcal{VO}_{AB_i}^{\tau}, \forall i \in \{1, \dots, m-1\}. \quad (22)$$

Reference [24] specifies that because the velocity obstacle is a truncated cone, for a finite time horizon τ , the origin of the velocity space always lies outside the velocity obstacle. ORCA_A^{τ} will therefore not be empty if the desired velocities of all agents are set to zero. A collision-free velocity v_A^{new} is then computed as

$$v_A^{\text{new}} = \underset{v \in \text{ORCA}_A^{\tau}}{\text{argmin}} \|v - v_A^{\text{pref}}\|. \quad (23)$$

III. PROPOSED METHOD

This section presents the main results of this paper and is divided into three subsections. Subsection III-A describes the disturbances and measurement uncertainty considered in this work. In subsection III-B, a methodology that ensures collision-free motion when uncertainties are present is proposed and formalized. An algorithm for collision-free multi-swarm coverage control in the presence of disturbances is introduced in subsection III-C.

A. Disturbance and Measurement Uncertainty

Consider a first-order system where a velocity control input u_i is applied to an agent i operating in the presence of a disturbance. Denote the velocity of the disturbance at the location x_i at time t as $v_{d(i,t)}$. Then, the kinematics are

$$\begin{aligned}\dot{x}_i &= v_i, \\ v_i &= u_i + v_{d(i,t)}.\end{aligned}\quad (24)$$

In this work, the measured disturbance velocity at the location x_i at time t is denoted as $v_{d(i,t)}^{meas}$. It is described by the true disturbance velocity plus an additive sensor bias $b_{d(i)}$ and time-dependent noise $e_{d(i,t)}$,

$$v_{d(i,t)}^{meas} = v_{d(i,t)} + b_{d(i)} + e_{d(i,t)}. \quad (25)$$

It is assumed that an estimate $\hat{b}_{d(i)}$ for $b_{d(i)}$ is available. We will describe the deviation of $\hat{b}_{d(i)}$ from $b_{d(i)}$ as

$$\delta b_{d(i)} = b_{d(i)} - \hat{b}_{d(i)}. \quad (26)$$

To obtain an estimate $\hat{v}_{d(i,t)}$ for $v_{d(i,t)}$ based on the measured value and the estimated sensor bias, let

$$\hat{v}_{d(i,t)} = v_{d(i,t)}^{meas} - \hat{b}_{d(i)}. \quad (27)$$

Inserting $v_{d(i,t)}^{meas}$ as defined in (25) into (27) yields

$$\hat{v}_{d(i,t)} = v_{d(i,t)} + b_{d(i)} + e_{d(i,t)} - \hat{b}_{d(i)}, \quad (28)$$

which using equation (26) leads to

$$\hat{v}_{d(i,t)} = v_{d(i,t)} + \delta b_{d(i)} + e_{d(i,t)}. \quad (29)$$

Let

$$\xi_{d(i,t)} = \delta b_{d(i)} + e_{d(i,t)}. \quad (30)$$

It is assumed that

$$\xi_{d(i,t)} \in \varepsilon_i \quad (31)$$

is bounded by an ellipsoid, where

$$\varepsilon_i = \{z \mid z^T P z \leq 1\} \quad (32)$$

for some given $P = P^T > 0$ and $z = [v_x \ v_y \ v_z]^T$. Equations (29) and (30) yield

$$\xi_{d(i,t)} = \hat{v}_{d(i,t)} - v_{d(i,t)}. \quad (33)$$

Given a desired velocity v_i^{pref} that is to be adopted, we will now design a velocity control input u_i that counteracts external disturbances based on their bounds. Assuming that sufficient control input to counteract these disturbances can always be achieved, consider

$$u_i = v_i^{pref} - \hat{v}_{d(i,t)}. \quad (34)$$

Inserting (34) into (24), we obtain

$$v_i = v_i^{pref} + v_{d(i,t)} - \hat{v}_{d(i,t)}. \quad (35)$$

Using (33) and (35) yields

$$v_i = v_i^{pref} - \xi_{d(i,t)}. \quad (36)$$

Subsection III-B addresses the effects of $\xi_{d(i,t)}$ by computing a new collision-free velocity v_i^{new} based on v_i^{pref} and ε_i .

B. Collision Avoidance with Disturbance Measurements

In this subsection, a methodology based on ORCA is proposed to account for bounded measurement uncertainty and guarantee collision-free motion. We use the alphabet to identify each agent i , i.e., $i = A, B, \dots$, to be consistent with the notation in reference [24] as presented in section II-B.

Consider the Minkowski sum of ε_A and ε_B which is

$$\varepsilon_{AB}^{sum} = \varepsilon_A + \varepsilon_B = \{\eta_A + \eta_B \mid \eta_A \in \varepsilon_A, \eta_B \in \varepsilon_B\}, \quad (37)$$

and translate the resulting set ε_{AB}^{sum} by v_{AB}^{pref} , which yields

$$\overline{\varepsilon_{AB}^{sum}} = \varepsilon_{AB}^{sum} + v_{AB}^{pref}. \quad (38)$$

Theorem 3. *Assume that the constraint (31) is satisfied for both $\xi_{d(A)}$ and $\xi_{d(B)}$. If the agents A and B apply control inputs u_A and u_B as defined in equation (34) with i replaced by A and B, respectively, based on given desired velocities v_A^{pref} and v_B^{pref} , then*

$$v_A - v_B \in \overline{\varepsilon_{AB}^{sum}}, \quad (39)$$

where v_A and v_B are given by equation (36) with i replaced by A and B, respectively.

Proof. From equation (36) with i replaced by A and B, respectively, we can write

$$\begin{aligned}v_A &= v_A^{pref} - \xi_{d(A)}, \\ v_B &= v_B^{pref} - \xi_{d(B)}.\end{aligned}\quad (40)$$

Subtracting v_B from v_A yields

$$v_A - v_B = v_A^{pref} - \xi_{d(A)} - (v_B^{pref} - \xi_{d(B)}), \quad (41)$$

which using equation (15) can be rewritten as

$$v_A - v_B = -\xi_{d(A)} + \xi_{d(B)} + v_{AB}^{pref}. \quad (42)$$

Since $\xi_{d(A)} \in \varepsilon_A$ and $\xi_{d(B)} \in \varepsilon_B$ from equation (31),

$$-\xi_{d(A)} + \xi_{d(B)} \in -\varepsilon_A + \varepsilon_B, \quad (43)$$

where

$$-\varepsilon_A = \varepsilon_A \quad (44)$$

due to ε_A being symmetric about the origin. Adding v_{AB}^{pref} on both sides, we obtain

$$-\xi_{d(A)} + \xi_{d(B)} + v_{AB}^{pref} \in -\varepsilon_A + \varepsilon_B + v_{AB}^{pref}. \quad (45)$$

Therefore, from equation (42) and (45),

$$v_A - v_B \in -\varepsilon_A + \varepsilon_B + v_{AB}^{pref}. \quad (46)$$

Using (44) allows us to rewrite equation (46) as

$$v_A - v_B \in \varepsilon_A + \varepsilon_B + v_{AB}^{pref}. \quad (47)$$

Equations (37), (38), and (47) yield (39). \square

Corollary 2. *Let A and B apply their control inputs u_A and u_B as defined in equation (34) with i replaced by A and B, respectively, based on given desired velocities v_A^{pref} and v_B^{pref} . Let v_A^{pref} and v_B^{pref} be constant for a time horizon τ .*

Assume that (31) is satisfied for both $\xi_{d(A)}$ and $\xi_{d(B)}$. Then A and B will not collide before τ units of time if

$$\overline{\varepsilon_{AB}^{sum}} \cap \mathcal{VO}_{AB}^\tau = \emptyset. \quad (48)$$

Proof. Using Theorem 3 we know that

$$v_A - v_B \in \overline{\varepsilon_{AB}^{sum}}. \quad (49)$$

Moreover, Theorem 1 states that a collision between A and B happens if and only if

$$v_A - v_B \in \mathcal{VO}_{AB}^\tau. \quad (50)$$

Thus, no collision occurs if and only if

$$v_A - v_B \notin \mathcal{VO}_{AB}^\tau, \quad (51)$$

which is the case when (48) is satisfied. \square

As a result of Corollary 2, we determine a vector w that translates $\overline{\varepsilon_{AB}^{sum}}$ outside of \mathcal{VO}_{AB}^τ . This is achieved by translating $\overline{\varepsilon_{AB}^{sum}}$ into a half-space π , which we define as

$$\pi = \{v \mid (v - p) \cdot n > 0\}, \quad (52)$$

where p is computed as

$$p = \operatorname{argmin}_{v \in \partial \mathcal{VO}_{AB}^\tau} \|v - v_{AB}^{pref}\|, \quad (53)$$

and n is the outward normal vector of $\partial \mathcal{VO}_{AB}^\tau$ at p . Notice that

$$\pi \cap \mathcal{VO}_{AB}^\tau = \emptyset. \quad (54)$$

We therefore solve

$$w = \begin{cases} \operatorname{argmin}_{\bar{w}} \|\bar{w}\| \\ \text{s.t. } (\overline{\varepsilon_{AB}^{sum}} + \bar{w}) \in \pi \end{cases}, \quad (55)$$

or, equivalently,

$$w = [(p - x^*) \cdot n] n, \quad (56)$$

where

$$x^* = \begin{cases} \min x^T x \\ \text{s.t. } x \in \overline{\varepsilon_{AB}^{sum}} \end{cases}. \quad (57)$$

Note that following the *Separating Hyperplane Theorem* (see reference [33], page 46) π is the upper half-space of the hyperplane that separates $\overline{\varepsilon_{AB}^{sum}} + w$ from \mathcal{VO}_{AB}^τ . A two-dimensional visualization of w is given in figure 2. The translation vector w is then used to define $ORCA_{AB}^\tau$ by equation (17). After obtaining the half-spaces of permitted velocities with respect to all other agents, A computes a set of collision-free velocities as in equation (20). The new velocity is obtained using equation (23).

Theorem 4. Let A and B apply their control inputs u_A and u_B as defined in equation (34) with i replaced by A and B, respectively, based on given velocities $v_A^{new} \in ORCA_{AB}^\tau$ and $v_B^{new} \in ORCA_{BA}^\tau$, where $ORCA_{AB}^\tau$ is computed as in equation (17) and $ORCA_{BA}^\tau$ is computed as in equation (18), with w as defined in equation (55) and where n is the outward normal vector of $\partial \mathcal{VO}_{AB}^\tau$ at p as defined in equation (53).

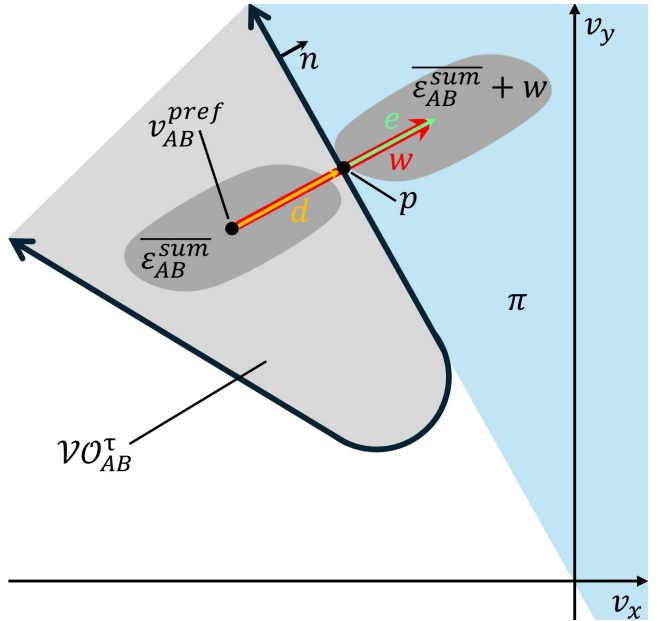


Fig. 2: Visualization of π

Let v_A^{new} and v_B^{new} be constant for a time horizon τ . Assume that the constraint (31) is satisfied for both $\xi_{d(A)}$ and $\xi_{d(B)}$. Then A and B do not collide before τ , i.e.,

$$v_A - v_B \notin \mathcal{VO}_{AB}^\tau. \quad (58)$$

Proof. Using equation (40) with v_A^{pref} replaced by v_A^{new} and v_B^{pref} replaced by v_B^{new} ,

$$v_A = v_A^{new} - \xi_{d(A)}, \quad (59)$$

$$v_B = v_B^{new} - \xi_{d(B)}. \quad (60)$$

Choosing new velocities $v_A^{new} \in ORCA_{AB}^\tau$ (equation (17)) and $v_B^{new} \in ORCA_{BA}^\tau$ (equation (18)) must satisfy

$$\left(v_A^{new} - \left(v_A^{pref} + \frac{1}{2}w \right) \right) \cdot n > 0 \quad (61)$$

and

$$\left(v_B^{new} - \left(v_B^{pref} - \frac{1}{2}w \right) \right) \cdot (-n) > 0. \quad (62)$$

Solving (59) and (60) for v_A^{new} and v_B^{new} , respectively, and inserting them in (61) and (62) yields

$$\left(v_A + \xi_{d(A)} - \left(v_A^{pref} + \frac{1}{2}w \right) \right) \cdot n > 0 \quad (63)$$

and

$$\left(v_B + \xi_{d(B)} - \left(v_B^{pref} - \frac{1}{2}w \right) \right) \cdot (-n) > 0. \quad (64)$$

Adding (63) and (64) gives

$$(v_A - v_B + \xi_{d(A)} - \xi_{d(B)} - v_A^{pref} + v_B^{pref} - w) \cdot n > 0. \quad (65)$$

Using (15) then yields

$$(v_A - v_B + \xi_{d(A)} - \xi_{d(B)} - v_{AB}^{pref} - w) \cdot n > 0. \quad (66)$$

Define

$$d = p - v_{AB}^{pref}. \quad (67)$$

Then d and n are collinear, i.e.,

$$d \parallel n \perp \partial \mathcal{VO}_{AB}^\tau. \quad (68)$$

Let

$$e = w - d, \quad (69)$$

where w is defined in (56). Using equations (67) and (69), (66) can be rewritten as

$$(v_A - v_B + \xi_{d(A)} - \xi_{d(B)} - (p + e)) \cdot n > 0. \quad (70)$$

Rearranging yields

$$(v_A - v_B - p) \cdot n > (e - \xi_{d(A)} + \xi_{d(B)}) \cdot n. \quad (71)$$

From (68), (56), and (69)

$$e = kn, \quad k > 0. \quad (72)$$

Since \mathcal{VO}_{AB}^τ is a closed set while π is an open set,

$$e \cdot n = \|e\| > 0. \quad (73)$$

Due to symmetry of ε_A and ε_B ,

$$\varepsilon_{AB}^{diff} = \varepsilon_A - \varepsilon_B = \varepsilon_A + (-\varepsilon_B) = \varepsilon_A + \varepsilon_B = \varepsilon_{AB}^{sum}, \quad (74)$$

where ε_{AB}^{sum} is defined in (37). Define an orthogonal coordinate system with origin at $v_{AB}^{pref} + w$ and with its primary axis along n . Consider the coordinate of $\xi_{d(A)} - \xi_{d(B)}$ along this axis, i.e., $(\xi_{d(A)} - \xi_{d(B)}) \cdot n$. Then there are two cases,

- 1) $(\xi_{d(A)} - \xi_{d(B)}) \cdot n \leq 0,$
- 2) $(\xi_{d(A)} - \xi_{d(B)}) \cdot n > 0.$

Using (73), for case 1 we can conclude that

$$\|e\| = e \cdot n > (\xi_{d(A)} - \xi_{d(B)}) \cdot n. \quad (75)$$

We will now prove by contradiction that this result still stands for case 2. To that aim, we first notice that, due to the symmetry of ε_{AB}^{sum} , for any $\xi_{d(A)} - \xi_{d(B)}$ in case 2 there is a corresponding point $\xi_{d(B)} - \xi_{d(A)}$ with negative coordinate along n , i.e.,

$$(\xi_{d(B)} - \xi_{d(A)}) \cdot n = -(\xi_{d(A)} - \xi_{d(B)}) \cdot n < 0. \quad (76)$$

Assume that there are $\xi_{d(A)}^*$ and $\xi_{d(B)}^*$ in case 2 such that $(\xi_{d(A)}^* - \xi_{d(B)}^*) \cdot n \geq \|e\|$. Then, this would imply that $\xi_{d(B)}^* - \xi_{d(A)}^* \in \mathcal{VO}_{AB}^\tau$ and therefore $\xi_{d(B)}^* - \xi_{d(B)}^* \notin \pi$, which violates the constraint in (55). Note that the constraint in (55) is on $\varepsilon_{AB}^{sum} + w$, which is a shifted version of ε_{AB}^{sum} . From case 1 and case 2 we can conclude that

$$e \cdot n > (\xi_{d(A)} - \xi_{d(B)}) \cdot n. \quad (77)$$

Rearranging equation (77) yields

$$(e - \xi_{d(A)} + \xi_{d(B)}) \cdot n > 0. \quad (78)$$

Using equations (71) and (78) leads to

$$(v_A - v_B - p) \cdot n > 0, \quad (79)$$

From (79) and (52),

$$v_A - v_B \in \pi. \quad (80)$$

Then, using equation (54) we conclude that (58) is satisfied. \square

Corollary 3. Consider m agents A, B_1, \dots, B_{m-1} operating within the same space. Let A choose $v_A^{new} \in ORCA_A^\tau$, where

$$v_A = v_A^{new} - \xi_{d(A)} \quad (81)$$

and $ORCA_A^\tau$ is defined in (20), with $ORCA_{AB_i}^\tau$ computed using w as defined in (55) and where n is the outward normal vector of $\partial \mathcal{VO}_{AB}^\tau$ at p as defined in (53). Then assuming that v_A^{new} and $v_{B_i}^{new}$ are constant for a time horizon τ and that the constraint (31) is satisfied for both $\xi_{d(A)}$ and $\xi_{d(B_i)}$, A will not collide with any other agent $B_i, i \in \{1, \dots, m-1\}$ that chooses a new velocity $v_{B_i}^{new} \in ORCA_{B_i A}^\tau$, i.e.,

$$v_A - v_{B_i} \notin \mathcal{VO}_{AB_i}^\tau, \forall i \in \{1, \dots, m-1\}, \quad (82)$$

where, from equation (36) with i replaced by B_i , we get

$$v_{B_i} = v_{B_i}^{new} - \xi_{d(B_i)}. \quad (83)$$

Proof. From the definition of $ORCA_A^\tau$ (equation (20)), assuming that v_A^{max} is finite,

$$ORCA_A^\tau \subset ORCA_{AB_i}^\tau, \forall i \in \{1, \dots, m-1\}. \quad (84)$$

Therefore, $v_A^{new} \in ORCA_A^\tau$ implies that $v_A^{new} \in ORCA_{AB_i}^\tau$. From Theorem 4, we know that $v_A^{new} \in ORCA_{AB_i}^\tau$ and $v_{B_i}^{new} \in ORCA_{B_i A}^\tau$ leads to (82). \square

C. Application to Multi-Swarm Coverage Control

The proposed algorithm to integrate the collision avoidance method presented in subsection III-B and coverage control with multiple swarms, is shown in table 1. We make the following assumptions:

- 1) All swarms use the same algorithm to cover the region and avoid other vehicles.
- 2) The computations are executed synchronously for all agents.
- 3) Group affiliation, as well as the radius of the sphere that defines a safety zone around an agent, are known for each agent.
- 4) Knowledge regarding the absolute positions of all other agents within the same swarm can be obtained through communication between vehicles.
- 5) The agents have sufficient sensing capabilities and communication within each swarm to determine the absolute positions of all agents from other swarms.
- 6) The input needed to counteract disturbances can always be achieved.

Remark 1. Note that assumptions 1-4 are commonly used in multi-agent systems [34]–[37]. For assumption 5, if there are at least 4 agents within one swarm and their relative positions are linearly independent, range measurements can be used to determine the positions of the agents from other

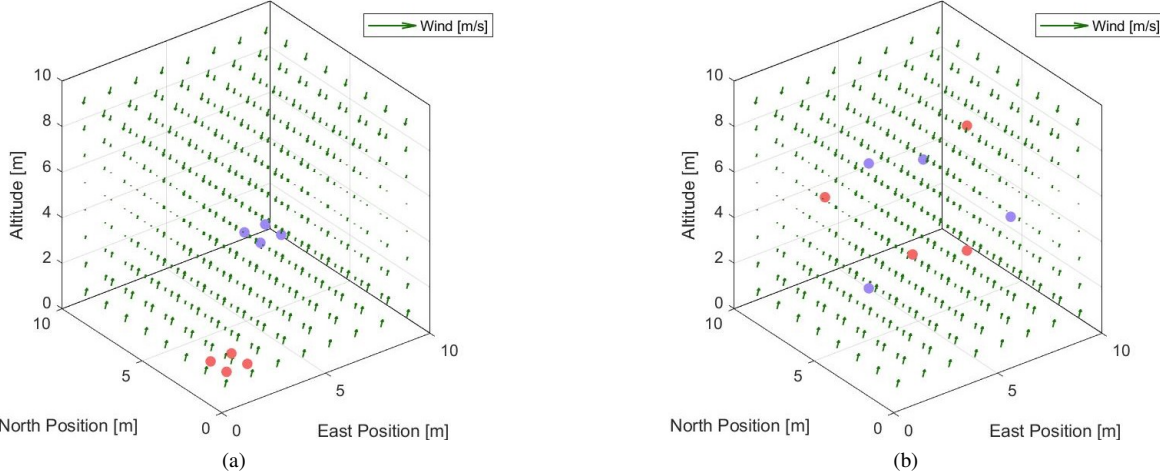


Fig. 3: Positions of the agents of swarm 1 (S1) and swarm 2 (S2) (a) at the beginning and (b) after 5 seconds.

Algorithm 1 Collision Avoidance for Multi-Swarm Coverage Control with Disturbance Measurement Uncertainty

Input: X, Q, D

Output: $u_{i,j}^{new}$

```

1:  $X, D \leftarrow \text{update}(X, D);$ 
2:  $x_{i,j} \leftarrow X_j(i);$ 
3:  $Edges_j, Vertices_j \leftarrow \text{voronoi}(X_j, Q);$ 
4:  $CM_{V_{i,j}} \leftarrow \text{centerOfMass}(Edges_j(i), Vertices_j(i));$ 
5:  $v_{i,j}^{pref} \leftarrow \text{desiredVelocity}(CM_{V_{i,j}}, x_{i,j}, k_{i,j});$ 
6:  $\hat{v}_{d(i,j)} \leftarrow \text{estimateDisturbances}(D);$ 
7: for all  $X_l \subset X, l = \{1, \dots, N\}$  do
8:    $Edges_l, Vertices_l \leftarrow \text{voronoi}(X_l, Q);$ 
9:   for all  $x_{k,l} \in X_l, \forall (k, l) \neq (i, j), k = \{1, \dots, m\}$  do
10:     $CM_{V_{k,l}} \leftarrow \text{centerOfMass}(Edges_l(k),$ 
11:     $Vertices_l(k));$ 
12:     $\hat{v}_{k,l}^{pref} \leftarrow \text{desiredVelocity}(CM_{V_{k,l}}, x_{k,l}, \hat{k}_{k,l});$ 
13:     $\mathcal{VO}_{(i,j)(k,l)}^\tau \leftarrow \text{velocityObstacle}(x_{i,j}, x_{k,l},$ 
14:     $r_{i,j}, r_{k,l}, \tau);$ 
15:     $v_{(i,j)(k,l)}^{pref} \leftarrow v_{i,j}^{pref} - \hat{v}_{k,l}^{pref};$ 
16:     $\varepsilon_{i,j}, \varepsilon_{k,l} \leftarrow \text{uncertaintyEllipsoids}(\xi_{d(i,j)}, \xi_{d(k,l)});$ 
17:     $\varepsilon_{(i,j)(k,l)}^{sum} \leftarrow \varepsilon_{i,j} + \varepsilon_{k,l} + v_{(i,j)(k,l)}^{pref};$ 
18:     $ORCA_{(i,j)(k,l)}^\tau \leftarrow \text{halfspace}(\mathcal{VO}_{(i,j)(k,l)}^\tau,$ 
19:     $\varepsilon_{(i,j)(k,l)}^{sum}, v_{(i,j)(k,l)}^{pref});$ 
20:     $ORCA_{(i,j)(l)}^\tau \leftarrow \bigcap_{k=1}^m ORCA_{(i,j)(k,l)}^\tau;$ 
21:  end for
22:   $ORCA_{i,j}^\tau \leftarrow D(0, v_{i,j}^{max}) \cap \bigcap_{l=1}^{N-1} ORCA_{(i,j)(l)}^\tau;$ 
23: end for
24:  $v_{i,j}^{new} \leftarrow \text{newVelocity}(ORCA_{i,j}^\tau);$ 
25:  $u_{i,j}^{new} \leftarrow v_{i,j}^{new} - \hat{v}_{d(i,j)};$ 
26: return  $u_{i,j}^{new}$ 

```

swarms. Note that if assumption 6 is not satisfied, it is pointless to design a control input that counteracts disturbances.

The algorithm is run for each agent. The agent for which

the algorithm is run is denoted as agent i belonging to swarm j . This is indicated by the subscript i, j . Note that X contains the positions of all agents, while D contains the disturbance measurements.

IV. SIMULATIONS

To validate the results, this section shows simulations of the kinematics of two swarms of fully actuated UAVs that independently aim to cover a three-dimensional region subject to a wind field. The region to cover is defined as a cube with an edge length of 10 meters (m) and has a uniform density distribution. We define a coordinate system with the origin at one vertex of the cube and the axes pointing in the East (x), North (y), and Up (z) directions, parallel to the faces of the cube. Both swarms consist of four agents initially located at

- 1) $[(1, 1, 1), (2, 2, 1), (2, 1, 1), (1, 2, 1)]$ m,
- 2) $[(9, 9, 1); (8, 8, 1); (8, 9, 1); (9, 8, 1)]$ m,

as illustrated in figure 3a. The maximum speed is set to 5 meters per second (m/s) for all agents. We define the wind field as $F(x, y, z) = (4 - z, 4 - z, 0)$ m/s, which corresponds to shear wind. For the wind measurement, the ellipsoid ε_i that bounds $\xi_d(i, t) = \delta b_d(i) + e_{d(i,t)}$ is defined by its semi-major axis $a = 0.15v_{d(i,t)}$ which is aligned with the direction of the wind and the two perpendicular semi-minor axes b and c with norms $\|b\| = \|c\| = \|0.005v_{d(i,t)}\|$. The time horizon is chosen to be $\tau = 1$ second (s), and the time step is $T = 0.01$ s. Figure 3b shows the locations of the agents after 5s, which is after the agents reach their final destinations. It can be seen that the agents from each swarm spread out during the simulation to cover the region. In particular, after 5s, the volume of the Voronoi cells of all agents is within 0.001% of $250m^3$. Since $250m^3$ is the total volume of the region to be covered divided by 4, which is the number of agents per swarm, this indicates that locally optimal coverage is achieved by both swarms. Furthermore, throughout the entire simulation, no collision occurred.

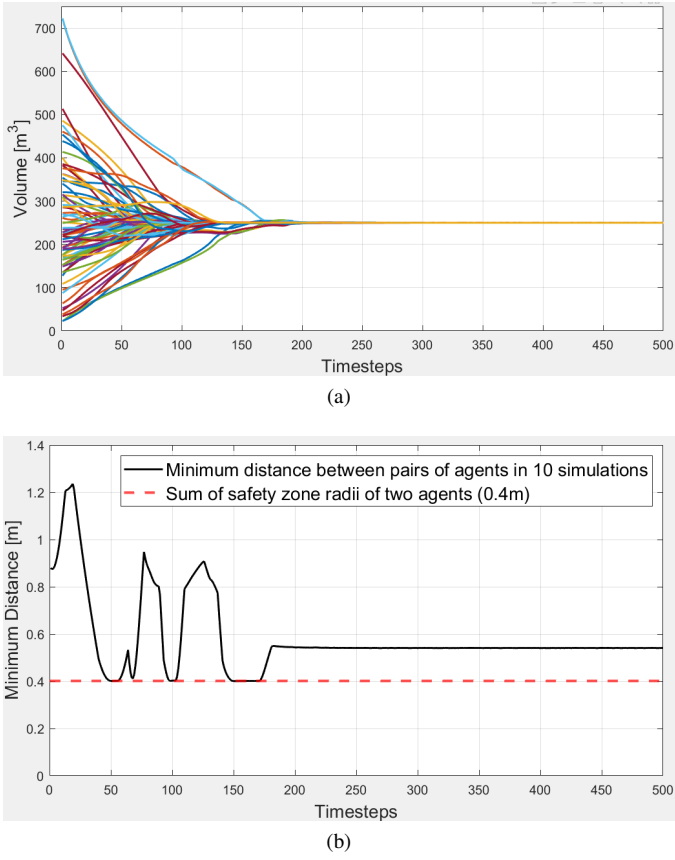


Fig. 4: Volume of Voronoi cells of each agent (a) and distance between each pair of agents from different swarms (b)

Figure 4 summarizes the results of 10 simulation runs for the same parameters, but with the agents starting from random initial positions. In figure 4a, the volume of the Voronoi cell of each agent is plotted over time. It can be seen that at the beginning, some agents cover a large volume, while others have less volume to cover. However, at the end of all simulations, the volumes of the Voronoi cells of all agents converge to 250m^3 , which suggests locally optimal coverage in all simulations. Moreover, figure 4b visualizes the minimum of the distance between each pair of agents belonging to different swarms at each timestep during all 10 simulations. Since the minimum distance never falls below the sum of the radii of the safety zones of two agents (0.4m), we can conclude that no collision occurs. These results demonstrate the effectiveness of the proposed methodology and algorithm, as well as their applicability to real-world scenarios.

V. CONCLUSIONS

This paper introduced a collision avoidance methodology for multi-agent systems. The method specifically accounts for bounded disturbances and uncertainty in their measurements, which makes it applicable to real-world environments. Since guarantees for collision-free motion in coverage control with only one swarm do not hold for the multi-swarm case, an algorithm was presented that introduces the

use of the proposed methodology for collision-free motion in multi-swarm coverage control. Collision avoidance is formally guaranteed. Simulations showed that using the new algorithm, both collision-free motion and locally optimal coverage can be achieved by multiple swarms operating within a three-dimensional region.

REFERENCES

- [1] K. Schmidt and L. Rodrigues, "Collision-free multi-agent coverage control for non-cooperating swarms: Preliminary results," 2024. [Online]. Available: <https://arxiv.org/abs/2411.08190>
- [2] J. Cortes, S. Martinez, T. Karatas, and F. Bullo, "Coverage control for mobile sensing networks," *IEEE Transactions on Robotics and Automation*, vol. 20, no. 2, pp. 243–255, 2004.
- [3] J. Cortés, S. Martínez, and F. Bullo, "Spatially-distributed coverage optimization and control with limited-range interactions," <http://dx.doi.org/10.1051/cocv:2005024>, vol. 11, 01 2004.
- [4] S. Lloyd, "Least squares quantization in pcm," *IEEE Transactions on Information Theory*, vol. 28, no. 2, pp. 129–137, 1982.
- [5] M. Moarref and L. Rodrigues, "An optimal control approach to decentralized energy-efficient coverage problems," *IFAC Proceedings Volumes*, vol. 47, no. 3, pp. 6038–6043, 2014, 19th IFAC World Congress. [Online]. Available: <https://www.sciencedirect.com/science/article/pii/S1474667016425577>
- [6] M. Di Perna and L. Rodrigues, "Distributed backstepping coverage control for multi-agents moving on a plane," in *2017 IEEE 56th Annual Conference on Decision and Control (CDC)*, 2017, pp. 1590–1595.
- [7] M. T. Nguyen, L. Rodrigues, C. S. Maniu, and S. Olaru, "Discretized optimal control approach for dynamic multi-agent decentralized coverage," in *2016 IEEE International Symposium on Intelligent Control (ISIC)*, 2016, pp. 1–6.
- [8] F. C. Siri, Y. Bai, and M. Svinin, "Safe coverage control for multi-agent systems," in *2023 62nd Annual Conference of the Society of Instrument and Control Engineers (SICE)*, 2023, pp. 1394–1399.
- [9] Z. Ma, J. You, Y. Zhang, Y. Cheng, and J. Shao, "Reinforcement learning-based dynamic coverage control of multi-rotor uavs with safety priority," *IEEE Transactions on Automation Science and Engineering*, vol. 22, pp. 17474–17485, 2025.
- [10] Y. Bai, Y. Wang, M. Svinin, E. Magid, and R. Sun, "Adaptive multi-agent coverage control with obstacle avoidance," *IEEE Control Systems Letters*, vol. 6, pp. 944–949, 2022.
- [11] Y. Yang, Y. Liang, and Y. Zhao, "An analytical solution for obstacle avoidance in cooperative area coverage using UAV swarms," in *2024 36th Chinese Control and Decision Conference (CCDC)*, 2024, pp. 2432–2437.
- [12] C. Song and Y. Fan, "Coverage control for mobile sensor networks subject to bounded measurement errors," in *2020 39th Chinese Control Conference (CCC)*, 2020, pp. 4864–4869.
- [13] J. Chen and P. Dames, "Distributed and collision-free coverage control of a team of mobile sensors using the convex uncertain voronoi diagram," in *2020 American Control Conference (ACC)*, 2020, pp. 5307–5313.
- [14] Y. Bai, Y. Wang, X. Xiong, J. Song, and M. Svinin, "Safe adaptive multi-agent coverage control," *IEEE Control Systems Letters*, vol. 7, pp. 3217–3222, 2023.
- [15] R. Haghghi and C. Cheah, "Multi-group coordination control for robot swarms," *Automatica*, vol. 48, no. 10, pp. 2526–2534, 2012. [Online]. Available: <https://www.sciencedirect.com/science/article/pii/S0005109812002658>
- [16] F. Sharifi, "Cooperative coverage control of multi-agent systems," Ph.D. dissertation, Concordia University, September 2014, unpublished. [Online]. Available: <https://spectrum.library.concordia.ca/id/eprint/979009/>
- [17] G. M. Atmç, D. M. Stipanović, and P. G. Voulgaris, "A swarm-based approach to dynamic coverage control of multi-agent systems," *Automatica*, vol. 112, p. 108637, 2020. [Online]. Available: <https://www.sciencedirect.com/science/article/pii/S0005109819304984>
- [18] Q. Wang and H. Zhang, "A self-organizing area coverage method for swarm robots based on gradient and grouping," *Symmetry*, vol. 13, no. 4, 2021. [Online]. Available: <https://www.mdpi.com/2073-8994/13/4/680>

- [19] F. Abbasi, A. Mesbahi, and J. Mohammadpour Velni, "A team-based approach for coverage control of moving sensor networks," *Automatica*, vol. 81, pp. 342–349, 2017. [Online]. Available: <https://www.sciencedirect.com/science/article/pii/S0005109817302108>
- [20] B. Cheng, M. He, Z. Zhu, B. He, and J. Chen, "Development and application of coverage control algorithms: A concise review," *IEEE Transactions on Automation Science and Engineering*, vol. 22, pp. 14 906–14 927, 2025.
- [21] P. Fiorini, "Motion planning in dynamic environments using velocity obstacles," *The International Journal of Robotics Research*, vol. 17, pp. 760–772, 07 1998.
- [22] J. van den Berg, M. Lin, and D. Manocha, "Reciprocal velocity obstacles for real-time multi-agent navigation," in *2008 IEEE International Conference on Robotics and Automation*, 2008, pp. 1928–1935.
- [23] S. J. Guy, J. Chhugani, C. Kim, N. Satish, M. Lin, D. Manocha, and P. Dubey, "Clearpath: highly parallel collision avoidance for multi-agent simulation," in *Proceedings of the 2009 ACM SIGGRAPH/Eurographics Symposium on Computer Animation*, ser. SCA '09. New York, NY, USA: Association for Computing Machinery, 2009, p. 177–187. [Online]. Available: <https://doi.org/10.1145/1599470.1599494>
- [24] J. van den Berg, S. J. Guy, M. Lin, and D. Manocha, "Reciprocal n-body collision avoidance," in *Robotics Research*, C. Pradalier, R. Siegwart, and G. Hirzinger, Eds. Berlin, Heidelberg: Springer Berlin Heidelberg, 2011, pp. 3–19.
- [25] F. Vesentini, R. Muradore, and P. Fiorini, "A survey on velocity obstacle paradigm," *Robotics and Autonomous Systems*, vol. 174, p. 104645, 02 2024.
- [26] J. Ellingson, E. Pitts, C. K. Peterson, K. Warnick, and T. McLain, "Uncertainty velocity obstacle avoidance for sUAS trajectory planning in a 2d plane," in *2020 IEEE Aerospace Conference*, 2020, pp. 1–11.
- [27] Z. Gyness and E. G. Szádeczky-Kardoss, "Motion planning for mobile robots using uncertain estimations about the environment," in *2020 23rd International Symposium on Measurement and Control in Robotics (ISMCR)*, 2020, pp. 1–6.
- [28] E. J. Rodríguez-Seda, D. M. Stipanović, and M. W. Spong, "Collision avoidance control with sensing uncertainties," in *Proceedings of the 2011 American Control Conference*, 2011, pp. 3363–3368.
- [29] S. Dergachev and K. Yakovlev, "Decentralized uncertainty-aware multi-agent collision avoidance with model predictive path integral," 2025. [Online]. Available: <https://arxiv.org/abs/2507.20293>
- [30] X. Zhang, J. Ma, Z. Cheng, M. Tomizuka, and T. H. Lee, "Velocity obstacle based risk-bounded motion planning for stochastic multi-agent systems," 2022.
- [31] S. Boddu, S. Suman, and S. De, "Impact of wind on UAV collision avoidance," in *ICC 2024 - IEEE International Conference on Communications*, 2024, pp. 2592–2597.
- [32] K. Schmidt, "Collision avoidance for non-cooperative multi-swarm coverage control with measurement uncertainty," Master's thesis, Concordia University, August 2025. [Online]. Available: <https://spectrum.library.concordia.ca/id/eprint/996175>
- [33] S. Boyd and L. Vandenberghe, *Convex optimization*. Cambridge university press, 2004.
- [34] W. Mao and T. Başar, "Provably efficient reinforcement learning in decentralized general-sum markov games," 2022. [Online]. Available: <https://arxiv.org/abs/2110.05682>
- [35] N. Bulling and M. Dastani, "Norm-based mechanism design," *Artificial Intelligence*, vol. 239, pp. 97–142, 2016. [Online]. Available: <https://www.sciencedirect.com/science/article/pii/S0004370216300789>
- [36] M. Braquet and E. Bakolas, "Vector field-based collision avoidance for moving obstacles with time-varying elliptical shape," 2022. [Online]. Available: <https://arxiv.org/abs/2207.01747>
- [37] D. Luo, Z. Fan, Z. Yang, and Y. Xu, "Multi-uav cooperative maneuver decision-making for pursuit-evasion using improved madrl," *Defence Technology*, vol. 35, pp. 187–197, 2024. [Online]. Available: <https://www.sciencedirect.com/science/article/pii/S221491472300301X>